Journal of Power Sources 210 (2012) 397–401

Contents lists available at SciVerse ScienceDirect

Journal of Power Sources

journal homepage: www.elsevier.com/locate/jpowsour

Short communication

Synthesis, characterization and electrochemical performance of Li_2FeSiO_4/C cathode materials doped by vanadium at Fe/Si sites for lithium ion batteries

Hao Hao, Junbo Wang, Jiali Liu, Tao Huang, Aishui Yu*

Department of Chemistry, Shanghai Key Laboratory of Molecular Catalysis and Innovative Materials, Institute of New Energy, Fudan University, Shanghai 200438, China

ARTICLE INFO

Article history:
Received 17 May 2011
Received in revised form
23 November 2011
Accepted 24 November 2011
Available online 2 December 2011

Keywords:
Lithium-ion battery
Iron silicate
Cathode material
Vanadium

ABSTRACT

Li_2FeSiO_4/C composites doped by vanadium at Fe/Si sites have been investigated as cathode materials for lithium ion batteries. Effects of vanadium substitution at different sites on the structure of Li_2FeSiO_4/C are examined by X-ray diffraction, X-photoelectron spectroscopy and scanning electron microscopy. XPS results show that the oxidation state of vanadium doped at Fe sites is +3, whereas is +5 when doped at Si sites. Electrochemical measurements show that the $Li_2FeSi_{0.9}V_{0.1}O_4$/C sample exhibits the best electrochemical performance with initial discharge capacity of 159 mAh g^{-1} and excellent cyclability with capacity of 145 mAh g^{-1} at 30th cycle, which can be ascribed to larger cell volume and higher lithium ion diffusion coefficient, however, the initial discharge of the $Li_2Fe_{0.9}V_{0.1}SiO_4$/C sample is only 90% of the undoped Li_2FeSiO_4, which can be attributed to the loss of Fe content.

1. Introduction

Since the demonstration of reversible electrochemical lithium insertion–extraction for Li_2FeSiO_4 by Nytén et al. [1], many works have been devoted to the study of this cathode material due to its low cost, environmental benignity and high theoretical capacity (166 mAh g^{-1}) [2–7]. To overcome its intrinsic low electrical conductivity of pristine Li_2FeSiO_4, considerable efforts have been made by carbon coating, particle size reduction, and super-valence ion doping [8–10].

Although isovalent cation doping can improve the electrochemical properties of Li_2FeSiO_4 by expanding its cell size and refining the particle size [11], aliovalent cation doping is considered to be a more effective way to modify its intrinsic properties such as electrical and ionic conductivities [12]. However, if an aliovalent cation could be indeed incorporated into the as-prepared materials, it might lead to vacancies at Li sites because of the need for charge balance [13]. Those vacancies might be expected to enhanced lithium ion conductivity, and therefore higher power capabilities. Although low-level doping at Fe sites could improve electrochemical properties of electrode materials, high-level doping at Fe sites could lead to lower capacity, because of reduction of Fe content [14].

Traditionally, super-valence ion doping at Fe sites is a normal way for phosphates and silicates type materials [15], however, doping at anion sites was proved an effective way for material improvement. Hong et al. prepared $LiFeP_{1-y}V_yO_4$ ($0 \le y \le 0.2$) under reducing condition, and demonstrated that 5% vanadium dopants could improve the electrochemical performance of $LiFePO_4$ [16]. Recently, substitution of SiO_4^{4-} with XO_4^{z-} (X = V, Ti or Al, Z = 3, 4 or 5) polyanions in Li_2MSiO_4 (M = Fe, Mn or Ni) was also reported [17,18]. The effect of VO_4^{3-} polyanions substitution for SiO_4^{4-} in the orthosilicate material Li_2FeSiO_4 was studied by Density Functional Theory (DFT), which demonstrated that its structure could be stable for <30% VO_4^{3-} substitution [18]. In this work, the effects of vanadium substitution at different sites on the characterization and electrochemical performance of Li_2FeSiO_4/C will be investigated.

2. Experimental

2.1. Preparation and characterization

All the samples (Li_2FeSiO_4/C, $Li_2Fe_{0.9}V_{0.1}SiO_4$/C, and $Li_2FeSi_{0.9}V_{0.1}O_4$/C) were prepared by sol–gel process. The stoichiometric amounts of $LiCH_3COO{\cdot}2H_2O$, $Fe(NO_3)_3{\cdot}9H_2O$, TEOS and NH_4VO_3 were used as precursors. First, $Fe(NO_3)_3{\cdot}9H_2O$ was dissolved in distilled water. Then, a saturated aqueous solution of citric acid was slowly added as chelating agent and carbon source under magnetic stirring at 60 °C. Subsequently solutions of $LiCH_3COO{\cdot}2H_2O$, NH_4VO_3 were added in turn, and an ethanol solution of TEOS was added dropwise. Then the mixture was stirred and refluxed at 80 °C for 24 h. The obtained solution was gently heated at 70 °C to remove the excess water and ethanol. The resulting gel precursor was dried at 100 °C in a vacuum oven

* Corresponding author. Tel.: +86 21 51630320; fax: +86 21 51630320.
E-mail address: asyu@fudan.edu.cn (A. Yu).

0378-7753/$ – see front matter © 2011 Elsevier B.V. All rights reserved.
doi:10.1016/j.jpowsour.2011.11.066

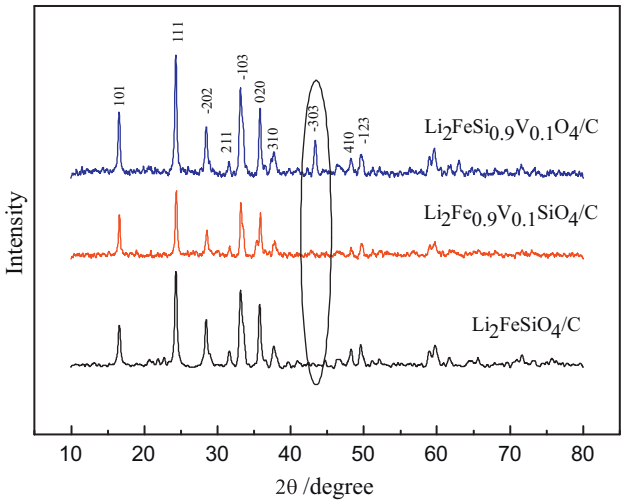

Fig. 1. XRD patterns of the as-prepared samples.

overnight. The dried precursor was sintered at 350 °C for 5 h, and then ground by a mortar and pestle, followed by further sintering at 650 °C for 10 h in an Ar–H_2 (5%) atmosphere.

The structures of the as-prepared materials were characterized by X-ray powder diffraction analysis (XRD, Bruker, 4 Advance, D8, model) using Cu Kα radiation (λ = 0.15406 nm). Lattice parameters from the materials were refined by the Rietveld analysis (Accelrys MS model 5.0). Morphological studies were conducted using a JEOL JMS 6390 scanning electron microscope. The chemical valence states of vanadium ions on the surface of the V-doped samples were investigated by using X-ray photoelectron spectroscopy (XPS, Perkin Elmer PHI-5000C ESCA system).

2.2. Electrochemical measurements

The electrochemical properties of the as-prepared samples were assessed using CR2016 coin cells. The composite electrodes were constructed by mixing the active materials, super P carbon black and polytetrafluoroethylene (PTFE) in the weight ratio of 70:20:10. The mixture was rolled into a thin sheet with uniform thickness and then pressed onto an aluminum mesh. The cathode was circular with a 10 mm diameter and dried under vacuum at 80 °C for 15 h. The coin cells were assembled in an argon-filled glove box with lithium pellet as anode, a Celgard 2300 sheet as separator and 1 M $LiPF_6$ in a mixed EC/DMC (1:1 in volume) solution as electrolyte. The charge–discharge measurements were carried out from 1.5 to 4.8 V (vs. Li^+/Li) using a Land Cycler (Wuhan Jinnuo Electronic Co. Ltd., China). The electrochemical impedance spectroscopy (EIS) measurements were performed on an electrochemical workstation (CHI 660A, CHI Company). The frequency was ranged from 0.001 to 100000 Hz with an amplitude of 0.005 V. All the tests were performed at room temperature.

3. Results and discussion

Fig. 1 shows XRD patterns of the as-prepared samples, which can be indexed to a monoclinic structure. It could be seen that the XRD patterns of $Li_2Fe_{0.9}V_{0.1}SiO_4/C$ is similar to that of the undoped Li_2FeSiO_4/C. However, there is noticeable difference between the XRD pattern of $Li_2FeSi_{0.9}V_{0.1}O_4/C$ and that of the undoped Li_2FeSiO_4/C for the peak around 43.3° (marked by ellipse), which could not be indexed by V_2O_5 or V but is similar to the literatures [10,19,20]. So, vanadium is considered to be incorporated into Li_2FeSiO_4/C at Si sites. Table 1 shows unit cell parameters of the as-prepared samples. From Table 1, we can see that the volume of the

Table 1
Unit cell parameters of the as-prepared samples by Rietveld refinement.

Sample	*a* (Å)	*b* (Å)	*c* (Å)	*β* (°)	*V* (Å^3)
Li_2FeSiO_4/C	8.2473	5.0144	8.2115	99.07	335.35
$Li_2Fe_{0.9}V_{0.1}SiO_4/C$	8.2425	5.0107	8.2005	98.96	334.55
$Li_2FeSi_{0.9}V_{0.1}O_4/C$	8.2354	5.0162	8.2474	98.93	336.58

undoped Li_2FeSiO_4/C is bigger than that of $Li_2Fe_{0.9}V_{0.1}SiO_4/C$, but smaller than that of $Li_2FeSi_{0.9}V_{0.1}O_4/C$, which could be explained by the different radius of cation. It is well known that the radius of V^{3+} (0.74 Å) is slightly smaller comparable to Fe^{2+} (0.76 Å) for the substitution of Fe^{2+} for V^{3+}, however, the radius of V^{5+} (0.59 Å) is extraordinarily larger than Si^{4+} (0.41 Å), which maybe bring the difference of XRD pattern around 43.3°. In details, the undoped

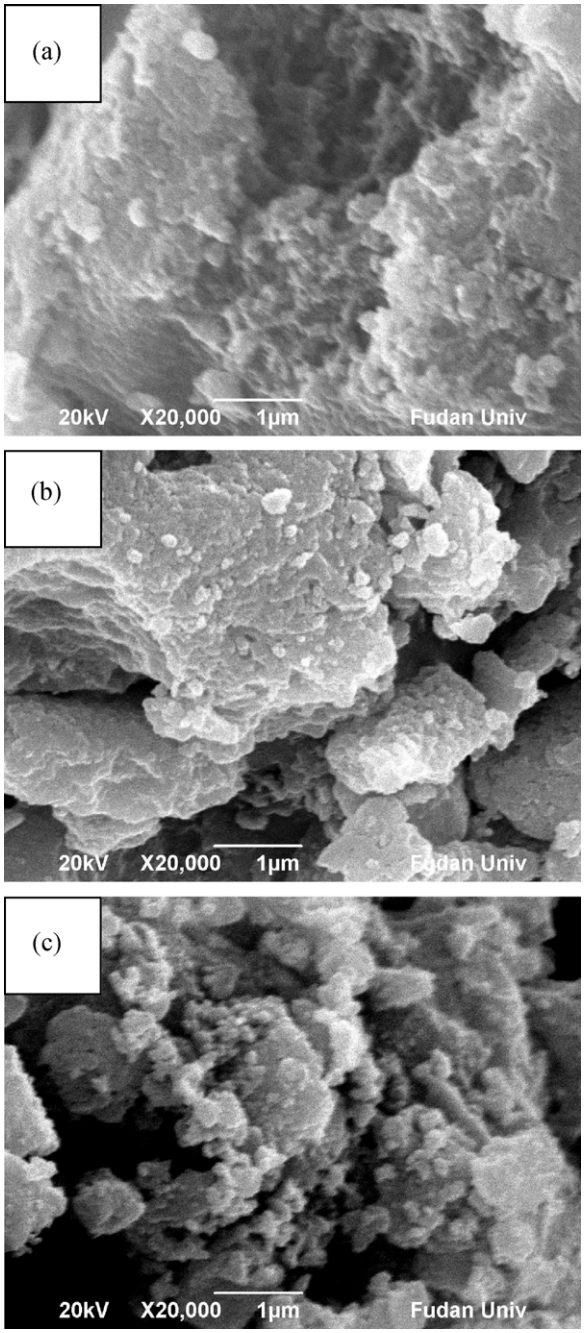

Fig. 2. SEM images of (a) Li_2FeSiO_4/C, (b) $Li_2Fe_{0.9}V_{0.1}SiO_4/C$ and (c) $Li_2FeSi_{0.9}V_{0.1}O_4/C$.

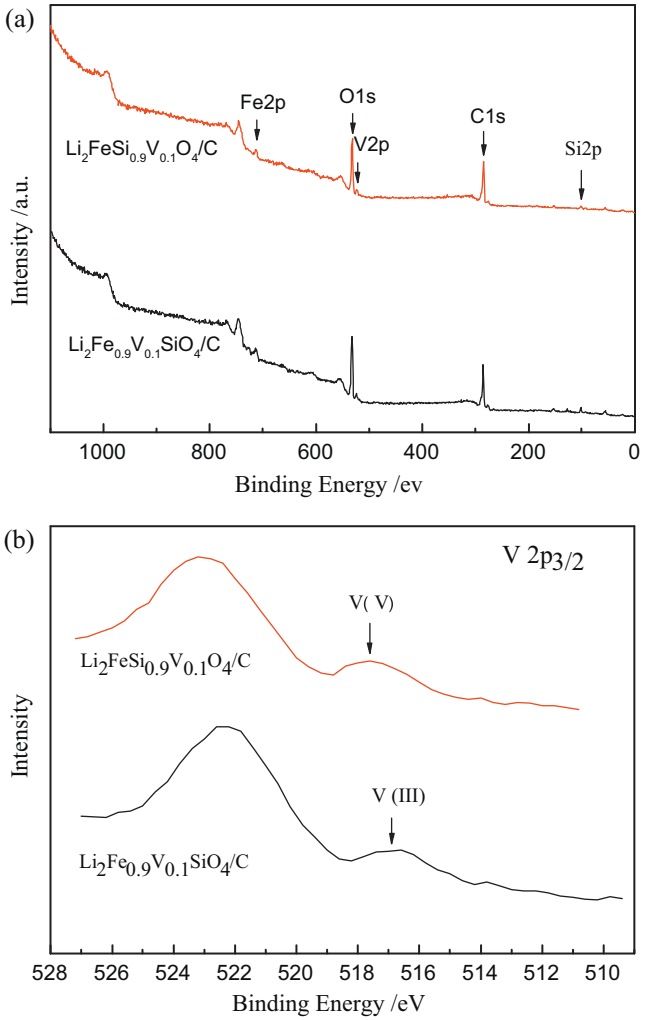

Fig. 3. XPS survey spectrum (a) and XPS core levels of V ($2p_{3/2}$) (b) in the V-doped samples at Fe/Si sites.

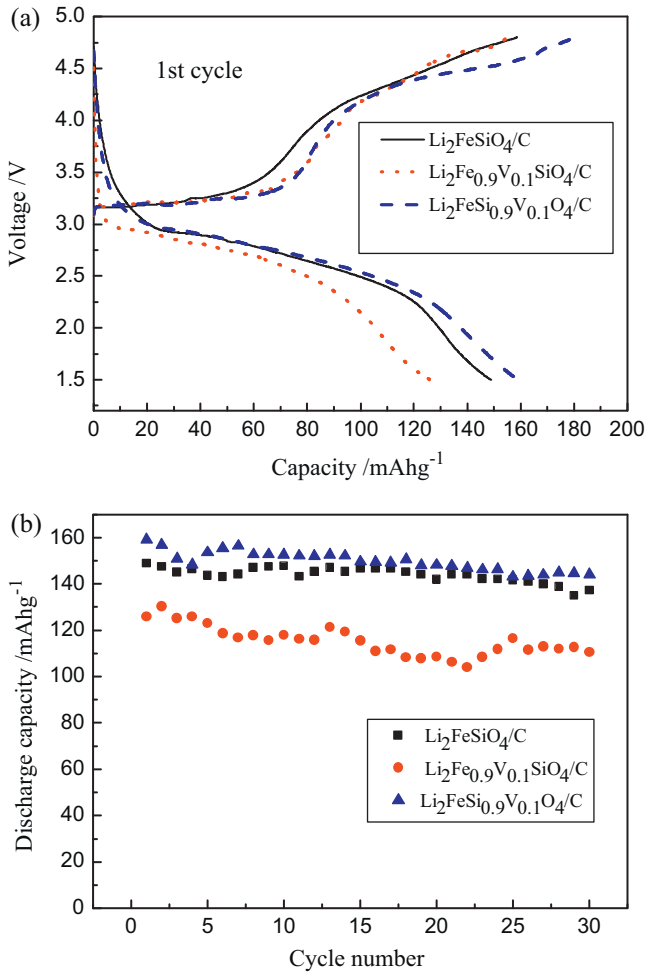

Fig. 4. (a) Initial charge–discharge curves and (b) cycling performances of the as-prepared samples.

Li_2FeSiO_4/C has the largest value of *a* axis, while $Li_2FeSi_{0.9}V_{0.1}O_4/C$ has the largest value of *b* and *c* axes. Interestingly, the lattice parameter β of both V-doped samples decreases a little, whether vanadium is incorporated into Fe sites or Si sites. Anyway, the similarity and slight difference of the cell parameter indicated that vanadium was sufficiently incorporated into the as-prepared materials at Fe/Si sites.

Fig. 2 shows SEM images of the as-prepared materials. There is no much difference on morphology, and all the samples are composed of agglomerated small primary particles about 100–200 nm.

XPS survey spectrum (a) and XPS core levels of V ($2p_{3/2}$) (b) in the V-doped samples at Fe/Si sites are shown in Fig. 3. The binding energy (BE) scales were calibrated by using the containment carbon (C 1s = 284.6 eV). For $Li_2Fe_{0.9}V_{0.1}SiO_4/C$, the V ($2P_{3/2}$) XPS core level fits to a single peak with a BE of 516.6 eV, which represents +3 [21,22]. However, for $Li_2FeSi_{0.9}V_{0.1}O_4/C$, the V ($2P_{3/2}$) XPS core level fits to a single peak with a BE of 517.6 eV, which represents +5 [23]. The different oxidation states of vanadium doping at Fe/Si sites were coincident with variation of relevant ionic radiuses and the stoichiometric amounts of precursors. In the case of Fe:Si:V was 0.9:1:0.1, vanadium was inclined to be reduced under reducing condition and incorporated into Fe^{2+} sites owing to their close radius sizes and charge-neutrality principle, because it was known that the radius of V^{3+} (0.74 Å) was extraordinarily close to that of Fe^{2+} (0.76 Å). And in the another case of Fe:Si:V was 1:0.9:0.1, VO_4^{3-} should be intended to incorporate into the sites of SiO_4^{4-} in the shape of polyanion, because both of V^{5+} and Si^{4+} were usually existed by VO_4 and SiO_4 tetrahedron [24], and it could not be reduced during sintering due to a mass of O atoms around V. Furthermore, vanadium of different super-valence states is incorporated into the as-prepared materials, which results in Li deficiency in view to the charge compensation mechanism, so the exact formulation of V-doped samples should be written as $Li_{1.9}Fe_{0.9}V_{0.1}SiO_4/C$ or $Li_{1.9}FeSi_{0.9}V_{0.1}O_4/C$. Anyway, the difference of vanadium valence state explains the variation of the lattice parameters; on the other hand, it is impossible that vanadium is not incorporated into the materials under the same preparing condition with the variation of vanadium valence state.

The initial charge–discharge curves at 1/16*C* of the as-prepared samples are shown in Fig. 4a. In the first cycle, all the samples show relatively large charge capacities at potentials above 4 V, which is attributed to the conjunct oxidation of $LiPF_6$ and transition metal [21], because the initial charge profile was slowly increasing curve, which could not to be solely connected to the oxidation of electrolyte. It not only could be driven by electrochemistry, but also had a chemical origin as a result of storage in the electrolyte, which resulted in the incomplete coverage surface-film formation. The formation of this film and oxidation of transition metal were main factors leading to the relatively large charge capacities above 4 V. It is also seen that 10% vanadium doping at Si sites reduces the polarization, but exactly opposite for doping at Fe sites, which is defined as the separation between charging and

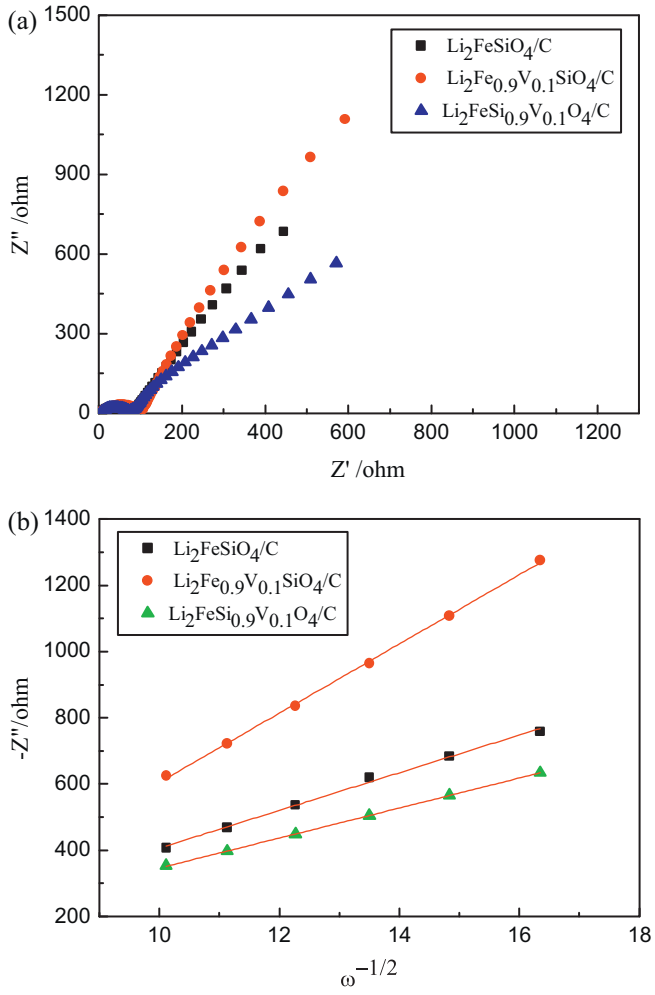

Fig. 5. Electrochemical impedance spectra of the as-prepared samples at open circuit potentials (a); the relationship curve between Z' and $\omega^{-1/2}$ in the low frequency (b).

discharging plateaus. However, the plateau for V^{3+}/V^{4+} or V^{4+}/V^{5+} is not observed for V-doped samples, which could be observed in the electrode $LiFe_{1-x}V_xPO_4$ [25]. Fig. 4b shows cycling performance of the as-prepared samples at 1/16C. $Li_2FeSi_{0.9}V_{0.1}O_4/C$ exhibits the largest capacity (159 mAh g^{-1}), which is higher than that of the pristine Li_2FeSiO_4/C (148 mAh g^{-1}), and remains 91% of the initial capacity after 30 cycles. The maximum of discharge capacity obtained in the second cycle for $Li_2Fe_{0.9}V_{0.1}SiO_4/C$ is in close to 90% of the initial capacity (maximum) of pristine Li_2FeSiO_4/C, which can be attributed to the loss of Fe content.

Since in our investigation, equal content of carbon was used as an electronic conductive agent, electrochemical impedance spectra measurements are carried out mainly to measure the lithium ion diffusion. As shown in Fig. 5a, each Nyquist plot is composed of a depressed semicircle and a straight line. It is well known that the intercept at the Z' axis in the high frequency corresponds to the Ohmic resistance of the electrolyte (R_e). The semicircle is related to the charge transfer resistance. The straight line in the low frequency is associated with lithium ion diffusion. The lithium ion diffusion coefficient could be calculated by Eq. (1):

$$D = \frac{R^2T^2}{2A^2n^4F^4C^2\sigma^2} \quad (1)$$

where R is the gas constant, T is the absolute temperature; A is the surface area of the cathode, n is the number of electrons per molecule during oxidation. F is the Faraday constant, C is the concentration of lithium ion, and σ is the Warburg factor which is relative with Z_{re}:

$$Z_{re} = RD + RL + \sigma\omega^{-1/2} \quad (2)$$

where ω is frequency. The relationship between Z_{re} and $\omega^{-1/2}$ in the low frequency are shown in Fig. 5b. The calculated lithium diffusion coefficient D ($cm^2\ s^{-1}$) of pristine Li_2FeSiO_4/C is $4.46 \times 10^{-14}\ cm^2\ s^{-1}$, which coincides with the previous reported [11]. The lithium diffusion coefficient of $Li_2FeSi_{0.9}V_{0.1}O_4/C$ ($6.91 \times 10^{-14}\ cm^2\ s^{-1}$) is larger than that of pristine Li_2FeSiO_4/C, but that of $Li_2Fe_{0.9}V_{0.1}SiO_4/C$ ($1.29 \times 10^{-14}\ cm^2\ s^{-1}$) is smallest, which could be related to the cell volume. These results also explain why the as-prepared cathode materials exhibit different electrochemical performance.

4. Conclusion

Li_2FeSiO_4/C cathode materials doped by vanadium at Fe/Si sites were prepared by sol–gel method. XRD and XPS analyses indicate that vanadium ions are successfully incorporated into Li_2FeSiO_4/C without altering its crystal structure. It is noted that vanadium doping at Fe/Si sites have different influence on the cell parameter: the cell volume is expanded when V-doping at Si sites, but shrunk when V-doping at Fe sites. The valence states of vanadium doping at Fe/Si sites are +3 or +5 respectively. $Li_2FeSi_{0.9}V_{0.1}O_4/C$ gives the best electrochemical performance, which can be explained by larger cell volume and higher lithium ion diffusion coefficient. On the other hand, $Li_2Fe_{0.9}V_{0.1}SiO_4/C$ exhibits poor performance, which may be due to the loss of Fe content.

Acknowledgments

The authors acknowledge funding supports from the Key Program of Basic Research of the Shanghai Committee of Science and Technology (10JC1401500), Science and Technology Commission of Shanghai municipality (08DZ2270500), China and the National High Technology Research and Development Program ("863" Program, No. 2009AA033701).

References

[1] A. Nytén, A. Abouimrane, M. Armand, T. Gustafsson, J.O. Thomas, Electrochem. Commun. 7 (2005) 156–160.
[2] R. Dominko, J. Power Sources 184 (2008) 462–468.
[3] A. Nytén, S. Kamali, L. Hanggstrom, T. Gustafsson, J.O. Thomas, J. Mater. Chem. 16 (2006) 2266–2272.
[4] R. Dominko, D.E. Conte, D. Hanzel, M. Gaberscek, J. Jamnik, J. Power Sources (2008) 842–847.
[5] R. Dominko, C. Sirisopanaporn, C. Masquelier, D. Hanzel, I. Arcon, M. Gaberscek, J. Electrochem. Soc. 157 (2010) A1309–A1316.
[6] M. Nadherna, R. Dominko, D. Hanzel, J. Reiter, M. Gaberscek, J. Electrochem. Soc. 156 (2009) A619–A626.
[7] Z.L. Gong, Y.X. Li, G.N. He, J. Li, Y. Yang, Electrochem. Solid-State Lett. 11 (2008) A60–A63.
[8] X.B. Huang, X. Li, H. Wang, Z. l. Pan, M. Qu, Z. l. Yu, Solid State Ionics 181 (2010) 1451–1455.
[9] T. Muraliganth, K.R. Stroukoff, A. Manthiram, Chem. Mater. 22 (2010) 5754–5761.
[10] S. Zhang, C. Deng, B.L. Fu, S.Y. Yang, L. Ma, Electrochim. Acta 55 (2010) 8482–8489.
[11] C. Deng, S. Zhang, S.Y. Yang, B.L. Fu, L. Ma, J. Power Sources 196 (2011) 386–392.
[12] M.R. Yang, W.S. Ke, S.h. Wu, J. Power Sources 165 (2007) 646–650.
[13] A.R. West, Chem. Rec. 6 (2011) 206–216.
[14] N. Recham, M.C. Cabanas, J. Cabana, C.P. Grey, J.C. Jumas, L. Dupont, M. Armand, J.M. Tarascon, Chem. Mater. 20 (2008) 6798–6809.
[15] H. Xie, Z.T. Zhou, Electrochim. Acta 51 (2006) 2063–2067.
[16] J. Hong, C.S. Wang, X. Chen, S. Upreti, M.S. Whittingham, Electrochem. Solid-State Lett. 12 (2009) A33–A38.
[17] M.E. Arroyo-de Dompablo, M. Armand, J.M. Tarascon, U. Amador, Electrochem. Commun. 8 (2006) 1292–1298.
[18] A. Liivat, J.O. Thomas, Comp. Mater. Sci. 50 (2010) 191–197.
[19] C. Deng, S. Zhang, S.Y. Yang, B.L. Fu, L. Ma, J. Electroanal. Chem. 644 (2010) 150–154.

[20] K. Karthikeyana, V. Aravindanb, S.B. Leea, I.C. Janga, H.H. Lima, G.J. Parkc, M. Yoshioc, Y.S. Lee, J. Alloys Compd. 504 (2010) 224–227.
[21] D. Ensling, M. Stjerndahl, A. Nytén, T. Gustafsson, J.O. Thomas, J. Mater. Chem. 19 (2009) 82–88.
[22] H.W. Liua, C.X. Cheng, X.T. Huang, J.L. Li, Electrochim. Acta 55 (2010) 8461–8465.
[23] J. Mendialdua, R. Casanova, Y. Barbaux, J. Electron. Spectrosc. Relat. Phenom. 71 (1995) 249–261.
[24] C. Sirisopanaporn, C. Masquelier, P.G. Bruce, A.R. Armstrong, R. Dominko, J. Am. Chem. Soc. 133 (2011) 1263–1265.
[25] X.J. Chen, G.S. Cao, X.B. Zhao, J.P. Tu, T.J. Zhu, J. Alloys Compd. 463 (2008) 385–389.